Experimental investigation of double-barrier SINIS (superconductor-insulator-normal-insulator-superconductor) structures

2000 J. Phys.: Condens. Matter 12 L1

(http://iopscience.iop.org/0953-8984/12/1/101)

J. Phys.: Condens. Matter **12** (2000) L1–L7. Printed in the UK PII: S0953-8984(00)06366-9

LETTER TO THE EDITOR

Experimental investigation of double-barrier SINIS (superconductor–insulator–normal–insulator–superconductor) structures

G Carapella, G Costabile and R Latempa

Unità INFM and Dipartimento di Fisica, Università di Salerno, I-84081 Baronissi, Italy

E-mail: giocar@physics.unisa.it (G Carapella)

Received 27 July 1999, in final form 4 November 1999

Abstract. Double-barrier $Nb/AlO_x/Al/AlO_x/Nb$ devices were fabricated and investigated in direct-current and alternating-current (ac) electromagnetic fields. The occurrence of current singularities and of the ac Josephson effect at $T = 4.2$ K are demonstrated. In a three-terminal configuration, a transistor-like behaviour of the structure is also observed.

In recent years SINIS junctions have attracted considerable attention [1–9] (here, S, I, and N denote a superconducting, an insulating, and a normal-metal layer, respectively). The investigation of such devices has focused mainly on non-equilibrium properties, the proximity effect, and Andreev reflection. Much experimental work [2, 5–8] was done with $Nb/AlO_x/Al/AlO_x/Nb$ double-barrier devices to explore their potential for application in superconductive electronics. The occurrence of dc supercurrent at $T = 4.2$ K, indirect evidence for an ac Josephson effect (Fiske modes) at $T < 4.2$ K, a non-hysteretic behaviour, and $I_C R_N \sim 0.5$ mV have already been demonstrated for these structures.

In this letter we report new experimental results on $Nb/AlO_x/Al/AlO_x/Nb$ structures. In particular, at $T = 4.2$ K, we have demonstrated:

(a) a dc Josephson effect, though we used a rather thick intermediate Al layer (≈30 nm);
(b) direct evidence of an ac Josephson effect—namely, the presence of Fiske singularities in a magnetic field originated by the Josephson current oscillation at $V \neq 0$, and both ordinary and zero-crossing Shapiro steps induced by microwaves;
(c) half-integer Shapiro steps;
(d) the presence of current singularities (named ZFSs in the following) in zero and non-zero dc magnetic field that show a peculiar behaviour under the influence of an applied microwave field;
(e) a transistor-like behaviour of the device when analysed in a three-terminal configuration.

The rich dynamics observed suggests that the structure cannot be regarded merely as two series-biased SIS′ junctions.

To fabricate the $Nb/AlO_x/Al/AlO_x/Nb$ structure, we used the procedure that [10] employed to make two stacked $Nb/AlO_x/Nb$ Josephson junctions with access to the intermediate electrode. The two devices on which we report here have double-overlap geometry (see the insets in figure 1(a) and figure 1(b)), and physical dimensions $L \times W = 600 \times 20\ \mu m^2$

0953-8984/00/010001+07$30.00

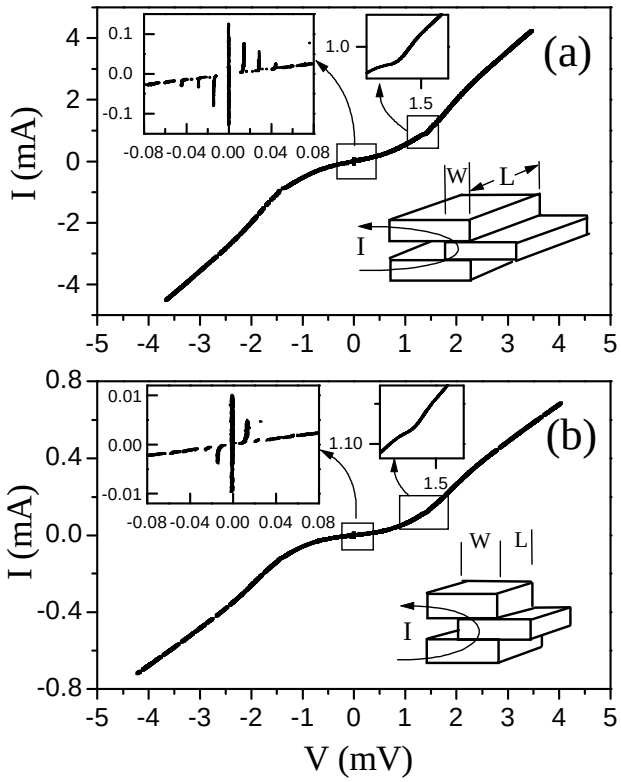

Figure 1. (a) The current–voltage characteristic of the SINIS structure. The geometry and biasing condition are shown in the inset. The magnifications show a knee typical of the proximity effect and a series of current singularities around the dc Josephson current. The IVC is recorded at $T = 4.2$ K, and at zero applied magnetic field. (b) As (a), but here the SINIS has a smaller area.

(device A) and $L \times W = 50 \times 50\ \mu\text{m}^2$ (device B). For both devices, the outer Nb electrodes were 300 nm thick, while the intermediate Al electrode was ≈30 nm thick.

Figure 1(a) shows the current–voltage characteristic (IVC) of device A, series biased. Though we used a relatively thick middle Al layer, the IVC shows a typical signature of the proximity effect, i.e., the knee at voltage $V = 2(\Delta_{\text{Nb}} - \Delta_{\text{Al}})/e \approx 1.45$ mV, where Δ_{Nb} is the energy gap of the outer Nb electrode and Δ_{Al} is the induced [2, 3, 5, 7] energy gap in the intermediate Al. The enlargement of the voltage region around $V = 0$ shows the dc Josephson current, $I_0 \approx 126\ \mu$A, and other current singularities, evenly spaced, with $\Delta V_{ZFS} \approx 15\ \mu$V. A similar IVC is exhibited by the smaller-area device B (figure 1(b)), with $I_0 \approx 10\ \mu$A and only a zero-field singularity at $V \approx 13\ \mu$V.

Figure 2 shows the characterization of the device A in the presence of a magnetic field. The magnetic field is applied perpendicular to the long dimension of the structure and in the plane of the junctions. The critical current I_0 follows a Fraunhofer-like pattern. This is typical [11] of rectangular, not electrically long, junctions having uniform critical current density J_0. From the pattern, we roughly estimate a magnetic thickness [11] of $d \approx 200$ nm from $d = \Phi_0/B_0 L$, where Φ_0 is the flux quantum, $B_0 \approx 0.175$ G is the first zero in figure 2(a), and L is the junction length. This value of d agrees with the values estimated from the pattern in a magnetic field of SINIS structures reported in the literature [6]. The Josephson penetration depth can also be

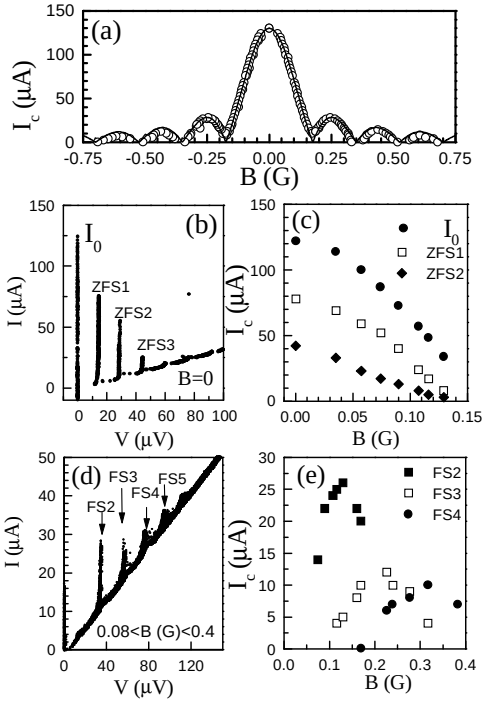

Figure 2. (a) The critical current of the A device as a function of the magnetic field. The experimental data follow the typical diffraction pattern: $I_c(B) = I_0|\sin(\pi B/B_0)/(\pi B/B_0)|$, with $I_0 = 126$ μA, and $B_0 = 0.175$ G. (b) Zero-field current singularities (ZFSs) recorded in the device. (c) Amplitudes of the ZFS1, ZFS2, and Josephson current I_0 as functions of the magnetic field. (d) Current singularities induced by a magnetic field and (e) their amplitudes as functions of the applied magnetic field.

estimated as $\lambda_J \approx 1200$ μm from [11]

$$\lambda_J = \sqrt{\Phi_0/2\pi\mu_0 J_0 d}$$

where $J_0 \approx 0.8$ A cm^{-2} is obtained from the I_0-value in figure 1(a).

Figure 2(b) shows the first three singularities, spaced with $\Delta V_{ZFS} \approx 15$ μV. These zero-field singularities, that we labelled as ZFS1, ZFS2, ..., have critical current decreasing with their order, a behaviour resembling that of the zero-field steps (ZFSs) accounting for oscillating fluxon motion in long-overlap junctions [12]. Also the magnetic field dependence of the critical current, shown in figure 2(c) for ZFS1 and ZFS2, resembles that of the ZFSs in long-overlap junctions. However, at the moment we cannot clearly identify the ZFSs shown in figure 2(b) as the steps observed in single or stacked junctions [13]. In fact, we are concerned with junctions that are electrically short ($l = L/\lambda_J \approx 0.5$ for the device A and $l = 0.04$ for the device B). Moreover, given that the electrical length should be estimated in a different manner (e.g., as in the framework of the inductive model [14]), it is not clear why a voltage spacing of the same order of magnitude is observed for two physical lengths that are quite different (we get $\Delta V_{ZFS} \approx 15$ μV for $L = 600$ μm and $\Delta V_{ZFS} \approx 13$ μV for $L = 50$ μm). This is not what should be expected in the case of singularities accounting for oscillating fluxon motion, which, instead, should exhibit a voltage spacing inversely proportional to the physical length of the junction [12].

In figure 2(d) there are shown current singularities, that we label as FS2, FS3, ..., induced by varying the magnetic field between $B = 0.08$ G and $B = 0.4$ G. They are evenly spaced, with $\Delta V_{FS} \approx 18\ \mu$V, and their critical current as a function of the magnetic field, shown in figure 2(e), is the one expected for cavity modes [11] (Fiske steps) generated by an ac Josephson effect.

In figure 3(a) is shown the behaviour of device B—but similar results are obtained for device A—under the influence of a microwave field at the frequency $\nu_{RF} = 8.60$ GHz. At low microwave level, the ZFS is only weakly modified. On increasing the amplitude of the rf signal, the dc Josephson current is destroyed, and the ZFS starts to extend, antisymmetrically, to the opposite side of the resistive branch. A further increase of the rf amplitude induces other branches of the ZFS family, and the negative antisymmetric branch grows further. Eventually, one can find ($P_{RF} = -16$ dBm in figure 3(a)) Shapiro steps at voltages $V_n = n\Phi_0\nu_{RF}$ ($n = -1, n = 1$) coexisting with both the branches of the ZFSs. We emphasize that this rf-induced antisymmetric current branch does not represent a voltage-locked state, and that it takes negative current values, a phenomenon that was never observed, either in junctions or in junction stacks.

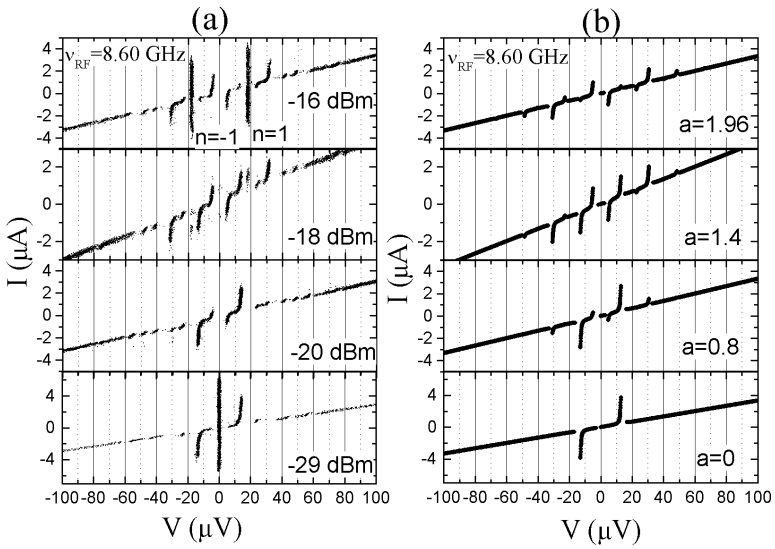

Figure 3. (a) Evolution of the ZFS of the B device under the effect of a microwave signal at frequency $\nu_{RF} = 8.60$ GHz of increasing (from the bottom to the top in the figure) power level P_{RF}. At $P_{RF} = -16$ dBm, also Shapiro steps are induced. (b) Evolution of the ZFS as described by relations (1) and (2).

A tentative explanation for these rf-induced antisymmetric branches could be based on the photon-assisted tunnelling mechanism. As is already known [15], the modification of the quasiparticle curve induced by a microwave field having frequency ν_{RF} and amplitude V_{RF} is reasonably well described by [16]

$$I(V) = \sum_{m=-\infty}^{\infty} J_m^2\left(\frac{qV_{RF}}{h\nu_{RF}}\right) I\left(V + m\frac{h\nu_{RF}}{q}\right) \tag{1}$$

where $J_m(a)$ is the mth-order Bessel function of the first kind, h is the Planck constant, q is the charge of the quasiparticle involved in the tunnelling, $I(V)$ is the current–voltage characteristic

in the absence of microwaves. For single-particle tunnelling ($q = e$, the charge of the electron) in ordinary tunnel junctions, relation (1) accounts for the steps [11,15] induced around the gap voltage, $V_k = (2\Delta/e + kh\nu_{RF}/e)$. Assuming that our ZFSs in the absence of microwaves can be ascribed to some quasiparticle tunnelling process, we expect relation (1) to describe their rf modification. A current–voltage curve that mimics the presence of a current singularity in the low-voltage region can be

$$I(V) = \frac{V}{R_{sg}} + \frac{\beta V}{(V^2 - V_s^2)^2 + (\beta V)^2} I_s \tag{2}$$

where R_{sg} is the subgap resistance, V_s is the apparent voltage, β is the damping, and I_s is proportional to the height of the current singularity. If we describe the ZFS in the device B with relation (2) and the corresponding rf-induced modification with relation (1), where we take $q = 2e$, we obtain the result shown in figure 3(b). As is apparent, the peculiarities of the experimental rf-induced modifications (in figure 3(a)) are all recovered. This suggests that the ZFSs are accounted for by quasiparticles of charge $q = 2e$. The relatively strong sensibility of the ZFSs to the dc magnetic field documented in figure 2(b) is reminiscent, on the other hand, of a Josephson nature of steps. The questions that arise are: are the quasiparticles involved Cooper pairs, and are they bound states? In our opinion this would be an intriguing topic for further experimental and theoretical study.

Zero-crossing, half-integer Shapiro steps are also observed in the devices. An example is shown in figure 4(a). These steps are enhanced if the rf frequency satisfies the empirical condition $\nu_{RF} = \Phi_0^{-1}\Delta_{ZFS}N$, where N is an integer. The presence of these half-integer steps

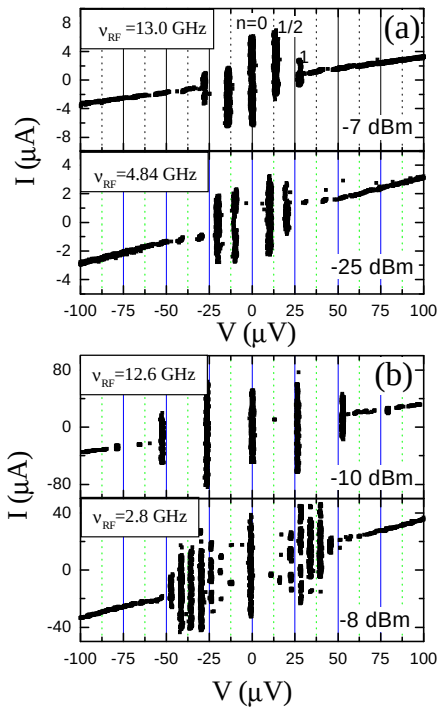

Figure 4. Ordinary and half-integer Shapiro steps induced by a microwave signal in the B device (in (a)) and in the A device (in (b)).

could be ascribed to a non-uniform current distribution induced at the particular frequency or to the presence of non-sinusoidal [1, 9] components in the current–phase relation. However, ordinary Shapiro steps are normally exhibited in the devices, as shown in figure 4. The results of figure 2(d) and figure 4 are direct evidence for ac Josephson effects in our SINIS structures.

Although our devices provide electrical access to the intermediate electrode, the configuration of our sample holder was not such as to allow us to perform four-contact measurements of the junctions independently. This is why we reported results obtained on series biasing the structure. However, in figure 5 we present a result obtained on biasing the devices in a three-terminal configuration (see the inset). The figure refers to the device A in a transistor-like configuration. As we see, the IVC curve of the device is controlled by the current I_B injected through the bottom junction. The most sensitive region of the I_S–V_S curve is that near the knee at $V_D \approx 2(\Delta_{\mathrm{Nb}} - \Delta_{\mathrm{Al}})/e$. In this region a small current gain $G = \Delta I_S/\Delta I_B \approx 1.4$ is obtained. Further investigations of this non-equilibrium effect could merit some interest as regards applications.

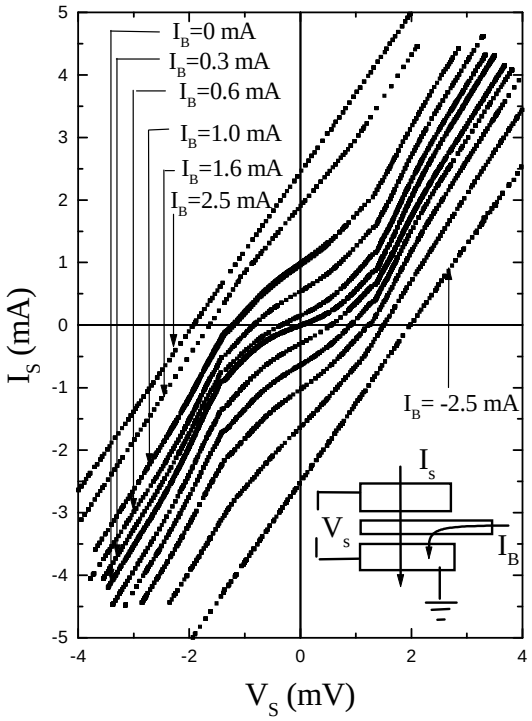

Figure 5. Modification of the current–voltage characteristic (the I_s–V_s characteristic; see the inset) by injection of a current I_B in the bottom junction of the device.

In summary, the $\mathrm{Nb/AlO}_x\mathrm{/Al/AlO}_x\mathrm{/Nb}$ structure investigated exhibits, at $T = 4.2$ K, ordinary dc and ac Josephson effects as well as some new effects. The behaviour of the observed zero-field current singularities under the influence of a dc or an ac electromagnetic field seems to identify their origin as quasiparticles with charge $q = 2e$. However, the precise identity of the quasiparticles involved should be further investigated. The presence of half-integer Shapiro steps collateral to ordinary Shapiro steps suggests the possibility of enhancement of non-sinusoidal corrections to the current–phase relation of the device at particular frequencies of the applied microwave signal. Finally, current injection experiments demonstrate that it

is relatively easy to obtain a non-equilibrium regime in the structure, with the possibility of transistor behaviour. This could be interesting for applications.

We wish to thank Professor N F Pedersen for fruitful discussions.

References

[1] Kupriyanov M Yu and Lukichev V F 1988 *Zh. Eksp. Teor. Fiz.* **94** 139 (Engl. Transl. 1988 *Sov. Phys.–JETP* **67** 1163)
[2] Blamire M G, Kirk E C G, Evetts J E and Klapwijk T M 1991 *Phys. Rev. Lett.* **66** 220
[3] Helsinga D R and Klapwijk T M 1993 *Phys. Rev.* B **47** 5157
[4] Volkov A F 1995 *Phys. Rev. Lett.* **74** 4730
[5] Capogna L and Blamire M G 1996 *Phys. Rev.* B **53** 5683
[6] Maezawa M and Shoji A 1997 *Appl. Phys. Lett.* **70** 3603
[7] Nevirkovets I P 1997 *Phys. Rev.* B **56** 832
[8] Nevirkovets I P, Ketterson J B and Lomatch S 1999 *Appl. Phys. Lett.* **74** 1624
[9] Nevirkovets I P and Shafranjuk S E 1999 *Phys. Rev.* B **59** 1311
[10] Carapella G 1999 *Phys. Rev.* B **59** 1407
[11] Barone A and Paterno' G 1982 *Physics and Applications of the Josephson Effect* (New York: Wiley)
[12] Pnevmatikos S and Pedersen N F 1993 *Future Directions of Nonlinear Dynamics in Physical and Biological Systems* ed P L Christiansen, J C Eilbeck and R D Parmentier (New York: Plenum)
[13] Carapella G, Costabile G, Petraglia A, Pedersen N F and Mygind J 1996 *Appl. Phys. Lett.* **69** 1300
[14] Sakai S, Bodin P and Pedersen N F 1993 *J. Appl. Phys.* **73** 2411
[15] Solymar L 1972 *Superconductive Tunnelling and Applications* (London: Chapman and Hall)
[16] Tien P K and Gordon J 1963 *Phys. Rev.* **129** 647